Supporting Information

Mechanistic investigation

of isopropanol conversion on alumina catalysts:

location of active sites for alkene / ether production

Kim Larmier,*[1,2,3] Céline Chizallet,*[3] Nicolas Cadran,[3] Sylvie Maury,[3] Johnny Abboud,[1,2] Anne-Félicie Lamic-Humblot, [1,2] Eric Marceau,*[1,2] Hélène Lauron-Pernot[1,2]

[1] Sorbonne Universités, UPMC Univ Paris 06, UMR 7197 CNRS, Laboratoire de Réactivité de Surface, F-75005, Paris, France.

[2] CNRS, UMR 7197 CNRS, Laboratoire de Réactivité de Surface, F-75005, Paris, France.

[2] IFP Energies nouvelles, Direction Catalyse et Séparation, Rond-Point de l'échangeur de Solaize, 69360 Solaize.

* E-mails: kim.larmier@upmc.fr, celine.chizallet@ifpen.fr, eric.marceau@upmc.fr

1- <u>XRD patterns</u>
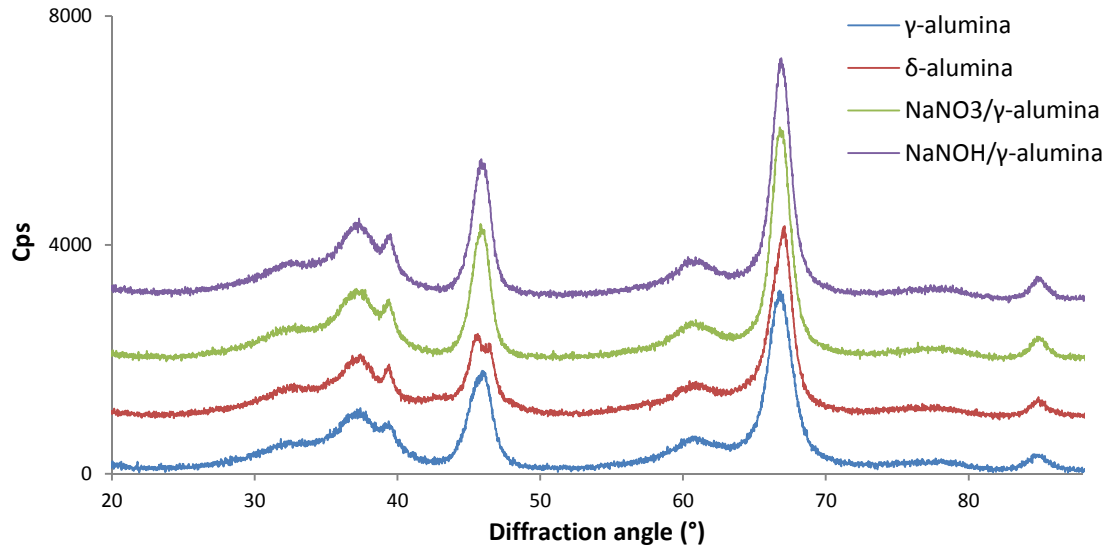
Figure S1. X-ray diffraction patterns of the four materials used throughout this study. For the sake of clarity, an offset has been applied to the diffractograms.

2- <u>Characterisation of the reactor</u>

The axial dispersion in a fixed-bed reactor is characterized by the axial Peclet number Pe_L, which in turn can be expressed as a function the Peclet number of inert particle Pe_m through the correlation

$$\frac{1}{Pe_L} = \frac{1}{\tau Pe_m} + \frac{1}{2}$$

where τ is the tortuosity of the catalytic bed ($\tau = 1.47$ in the case of a packing of spheres).[1] The Peclet number of inert particles Pe_m can be calculated through the formula

$$Pe_m = \frac{u d_P}{D_m}$$

where u is the interstitial axial velocity of the fluid, d_P the diameter of the particles (125-200 µm in our case ; we chose 160 µm for the calculation) and D_m the molecular diffusivity of the fluid (we considered the self-diffusivity value of nitrogen at 200 °C to be $4.65 \cdot 10^{-5}$ .m^2.s^{-1}).

Calculations yield Pe_L=0.24 for the highest flow rate investigated (60 mL.min^{-1}).

The number J of CSTR required to describe the axial dispersion of the reactor is given by the formula $J = 1 + Pe_L/2 = 1.12$, which we truncate to 1.The reactor can be assimilated to a single CSTR.

3- <u>Thermodynamic calculations</u>

For a given species i, $G(i,T,P)$ can be calculated through the formula **(S1)**

$$G(i,T,P) = E(i) + U_{vib}(i,T) + U_{rot}(i,T) + U_{trans}(i,T) + PV_m - T \times S_{vib}(i,T) - T \times S_{rot}(i,T) - T \times S_{trans}(i,T,P) \quad \textbf{(S1)}$$

The vibrational, rotational and translational enthalpic and entropic contributions for a gas phase molecule considered as an ideal gas can be calculated with equations **(S2) – (S3)**:

$$U_{vib}(i,T) = N_A \left[\sum_n \frac{1}{2} h\nu_n + \sum_n \frac{hc\nu_n \times exp\left(-\frac{h\nu_n}{k_BT}\right)}{1 - exp\left(-\frac{h\nu_n}{k_BT}\right)} \right] \quad \textbf{(S2)}$$

$$U_{trans}(i,T) + U_{rot,m}(i,T) + PV_m(i,T) = 4RT \quad \textbf{(S3)}$$

$$S_{vib}(i,T) = N_A k_B \left[\sum_n \frac{\frac{h\nu_n}{k_BT} \times exp\left(-\frac{h\nu_n}{k_BT}\right)}{1 - exp\left(-\frac{h\nu_n}{k_BT}\right)} - \sum_n \ln\left(1 - exp\left(-\frac{h\nu_n}{k_BT}\right)\right) \right] \quad \textbf{(S4)}$$

$$S_{rot}(i,T) = Nk_b \ln\left[\frac{\sqrt{\pi}}{\sigma} \left(\frac{8\pi^2 k_B T}{h^2}\right)^{\frac{3}{2}} \sqrt{A_{e,i} \times B_{e,i} \times C_{e,i}} \right] \quad \textbf{(S5)}$$

$$S_{trans}(i,T,P) = Nk_B \left(\frac{5}{2}\ln(T) - \ln(P) + \frac{5}{2}\ln(M_i) - 1{,}165 \right) \quad \textbf{(S6)}$$

where the vibrational contributions can be deduced from the calculated frequencies ν_n of the model (note that equation **(S3)** includes the zero point vibrational energy in its first term). $A_{e,i}$, $B_{e,i}$ and $C_{e,i}$ are the rotational constants of the molecule i, and M_i its molecular mass.[2,3]

For an adsorbed molecule or for a surface, the rotational and translational contributions are converted into vibration modes, so that the only remaining terms are the vibrational ones – that can be calculated using the equations **(S3)** and **(S5)** – and the electronic energy $E(i)$. For these phases, we also consider that the PV_m term is very small with regard to the energetic terms, and is therefore neglected, and thus we consider $H = U$ in this case.

In order to assess the uncertainty induced by the occurrence of additional imaginary frequencies on the calculated thermodynamic data, we evaluated these data on two cases, using three different methods for treating the imaginary frequencies:

- Method 1: the imaginary frequencies are turned into their real counterparts;
- Method 2: every wavenumber inferior to 50 cm^{-1} is set to 50 cm^{-1}, as proposed by Marin et al. [4,5]
- Method 3, adapted from Method 2: every wavenumber inferior to 25 cm^{-1} is set to 25 cm^{-1}.

The results are shown in Table S1. Adsorption or activation enthalpies are not affected by the choice of the method, as the vibrational component of the enthalpy (mainly ZPVE) essentially depends on the higher frequencies. Adsorption entropies show little dependence on the treatment method (with one notable exception), and activation entropies may vary by up to 14 J.K^{-1}.mol^{-1}, which at 200°C represent a Gibbs free energy offset of only 6.6 kJ.mol^{-1}. Note moreover that in most cases, the offset induced by the chosen method exhibits the same trend for the different reactions. Method 2 usually yields somewhat higher activation entropies than Methods 1 and 3, that lead to close results.

Table S1. Influence of the treatment of residual imaginary and very low frequencies on the calculated adsorption and activation parameters. Enthalpies are given in kJ.mol^{-1} and entropies are given in J.K^{-1}.mol^{-1}.

		Method 1	Method 2	Method 3
Formation of propene, E2, surface (100), site Al$_{Va}$	$\Delta_{ads}H°$	-121	-121	-121
	$\Delta_{ads}S°$	-186	-186	-186
	$\Delta_r H^{\ddagger}$	125	125	125
	$\Delta_r S^{\ddagger}$	-8	-4	-8
Formation of propene, E1$_{cb}$, surface (100), site Al$_{Va}$	$\Delta_{ads}H°$	-121	-121	-121
	$\Delta_{ads}S°$	-186	-186	-186
	$\Delta_r H^{\ddagger}$	147	147	147
	$\Delta_r S^{\ddagger}$	-43	-34	-45
Formation of ether, S$_N$2, surface (100), Al$_{Va}$/Al$_{Vb}$	$\Delta_{ads}H°$	-90	-90	-90
	$\Delta_{ads}S°$	-185	-191	-185
	$\Delta_r H^{\ddagger}$	178	178	178
	$\Delta_r S^{\ddagger}$	-39	-34	-29
Formation of ether, S$_N$2, surface (100), Al$_{Va}$/O$_{3a'}$	$\Delta_{ads}H°$	-62	-62	-62
	$\Delta_{ads}S°$	-146	-168	-147
	$\Delta_r H^{\ddagger}$	112	112	112
	$\Delta_r S^{\ddagger}$	-36	-22	-29

4- __Equilibrium calculations__

The thermodynamic limit of evolution of a system containing an initial partial pressure of 1.5 kPa of isopropanol (*i*PrOH) in nitrogen (total pressure of 1.0 atm) was evaluated as a function of the temperature (from 0 to 240 °C) using the Chemkin software and the Chemkin gas phase thermodynamic database.[6] The equilibrium isopropanol conversion is nearly 100 % on the whole investigated temperature range (Figure S2). Diisopropylether is the low-temperature product, while propene is obtained with a near 100 % selectivity above 150 °C. Thus, at 200 °C, the system should evolve to 100 % conversion of isopropanol with 100 % selectivity to propene once equilibrium conditions have been reached.
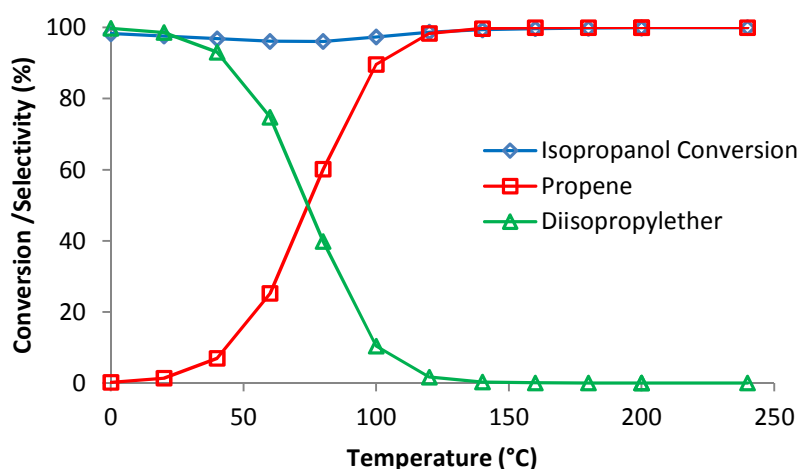

Figure S2. Equilibrium situation as a function of temperature, calculated using the Chemkin software with a total pressure of 1 bar and an initial isopropanol partial pressure of 1.5 kPa.

# 5- Kinetics experiments

5.1.   Steady-state conditions

Figure S3-(a) presents the evolution of isopropanol conversion with time-on-stream at a constant reaction temperature (200 °C) for 10 mg of pure γ-alumina diluted in SiC and activated at 450 °C. The initial isopropanol partial pressure was 1.5 kPa. Contact time was varied by varying the flow rate (*i. e.*, when the flow rate increased, contact time decreased and conversion was lowered, and *vice versa*). Under the initial flow rate (15.0 cc.min^{-1}, intermediate contact time), steady-state was achieved after a short induction period (roughly 45 min). After 2 h on stream, the flow rate was decreased to 8.0 cc.min^{-1} (high contact time); then increased to 47.0 cc.min^{-1} (low contact time); and back to its initial value. Conversion changed accordingly. After each change, steady-state was reached very quickly. It can be noted that the initial conversion (24 %) was fully recovered when the flow rate was changed back to 15.0 cc.min^{-1}. We left the system overnight under these reaction conditions. No deactivation of the catalyst was observed. We repeated the procedure the next day and obtained the same isopropanol conversion for each contact time. This experiment shows that in these reaction conditions and at 200 °C, water formed upon isopropanol dehydration does not accumulate on the surface. No poisoning effect is evidenced even for a conversion of 35%, indicating that if adsorbed on the active sites, water can be displaced by isopropanol from the gas-phase.

In a second series of measurements (Fig. S3-(b)), the catalyst was left under reaction flow and contact time was progressively increased by decreasing the isopropanol flow rate, leading to successive drops of the outlet isopropanol partial pressure (increasing conversions). It was checked that carbon balance between the inlet and the oulet was always higher than 97 % (experimental uncertainty may lead to a very slightly positive carbon balance in some cases) (Fig. S3-(c)). Isopropanol and reaction products do not accumulate on the alumina surface and desorb from the active in these reaction conditions and at 200 °C.
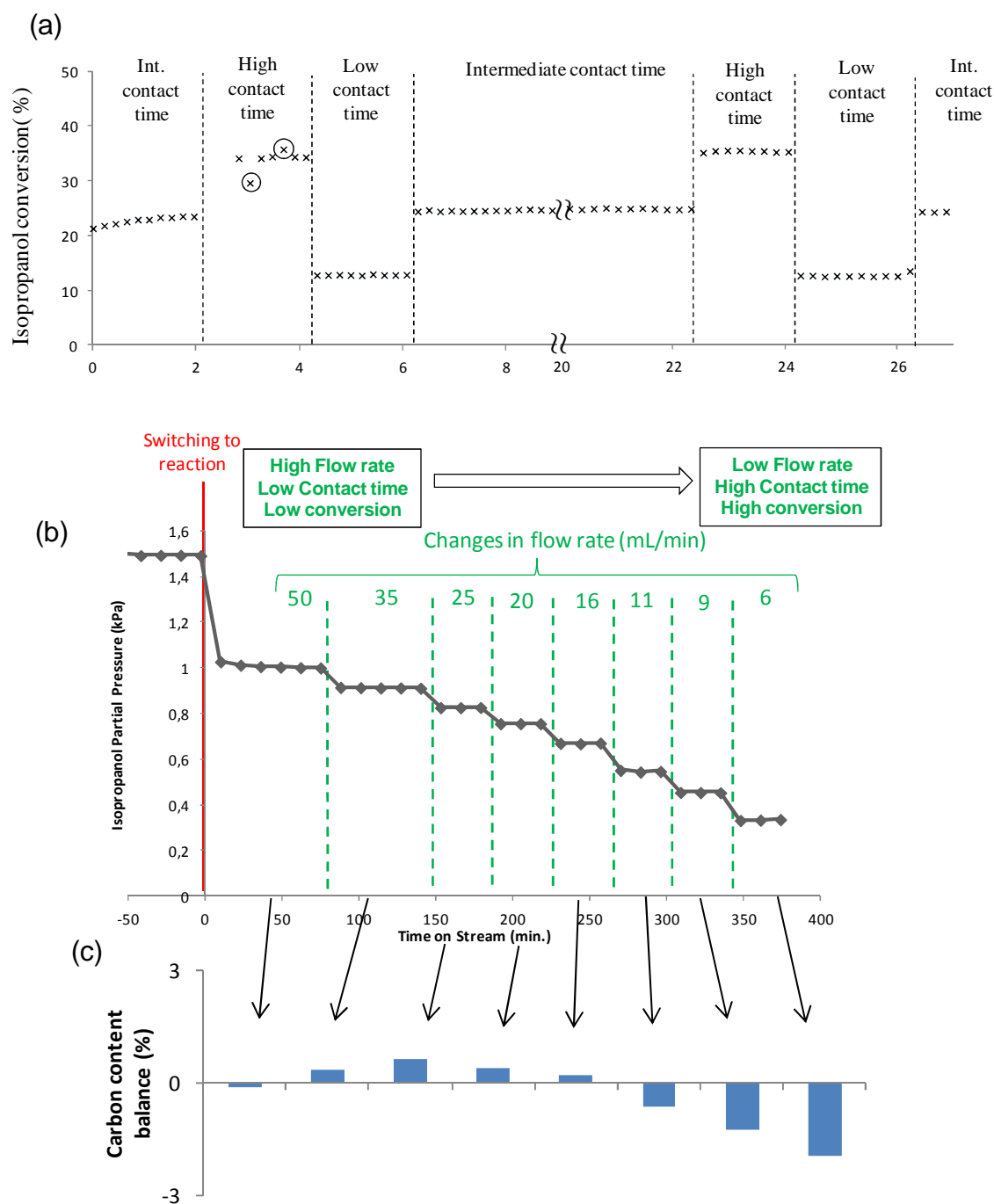
Figure S3. (a) Evolution of the isopropanol conversion with time-on-stream ($T_R = 200$ °C, initial $P_{iPrOH} = 1.5$ kPa, $m_{cata} = 4.0$ mg, activated at 450 °C for 3 h under N_2). At $t = 0$, the system was put under reaction conditions. Flow rate changes are marked with dotted lines. The encircled data points are related to instabilities in the flow rate regulation when the set value is low, and should not been considered. Intermediate contact time: $Q = 15.0$ cc.min^{-1}; high contact time: $Q = 8.0$ cc.min^{-1}; low contact time: $Q = 47.0$ cc.min^{-1}. (b) Typical set of experiments where contact time is progressively increased. (c) Corresponding carbon balance.
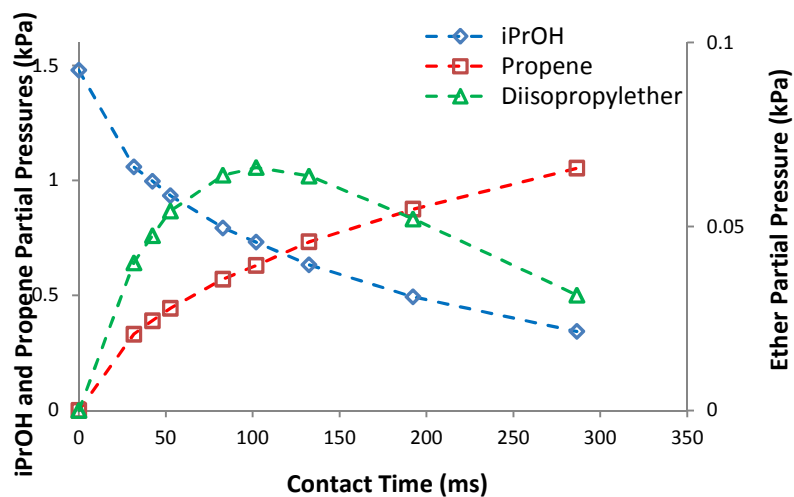
5.2.   <u>**Arrhenius plots**</u>

1000/T (K-1)
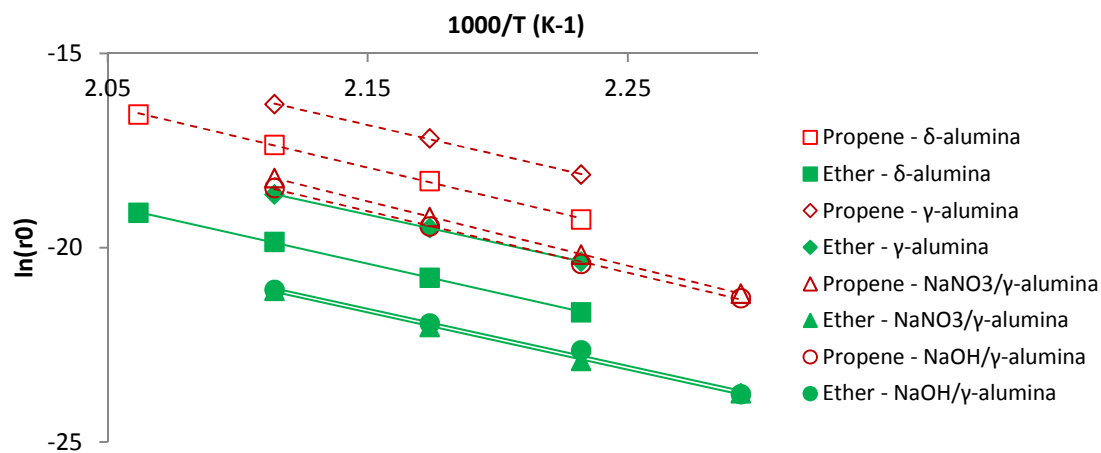
Figure S4. Arrhenius plots for the formation of ether and propene on the four investigated materials. r_0 is expressed in mol.m^{-2}.s^{-1}. Isopropanol conversion was kept below 8 %.
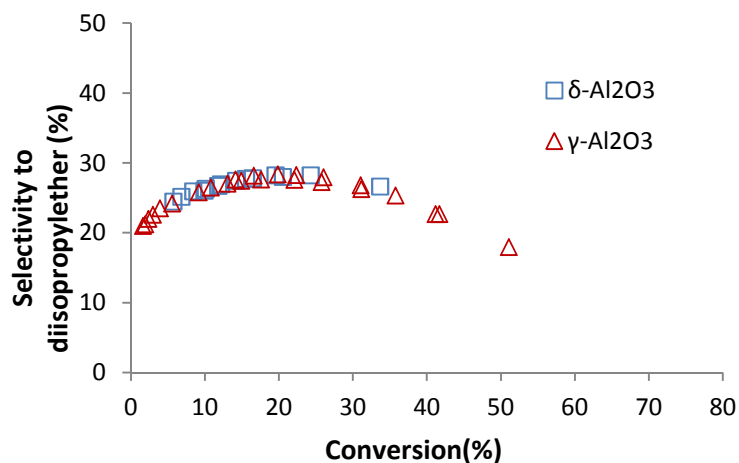
## 5.3.   <u>**δ-alumina**</u>

- Evolution of partial pressures with contact time

Figure S5. Partial pressures evolution on δ-alumina. T_R = 200 °C, P_{iPrOH} = 1.5 kPa, m_{cata} = 60 mg.

- Selectivity *vs.* conversion at 180 °C

Figure S6. Selectivity to diisopropylether *vs.* conversion plot monitored for a reaction temperature of 180 °C for the γ-alumina and δ-alumina samples. Initial P_{iPOH} = 1.5 kPa.

5.4. <u>Na-poisoned γ-alumina</u>
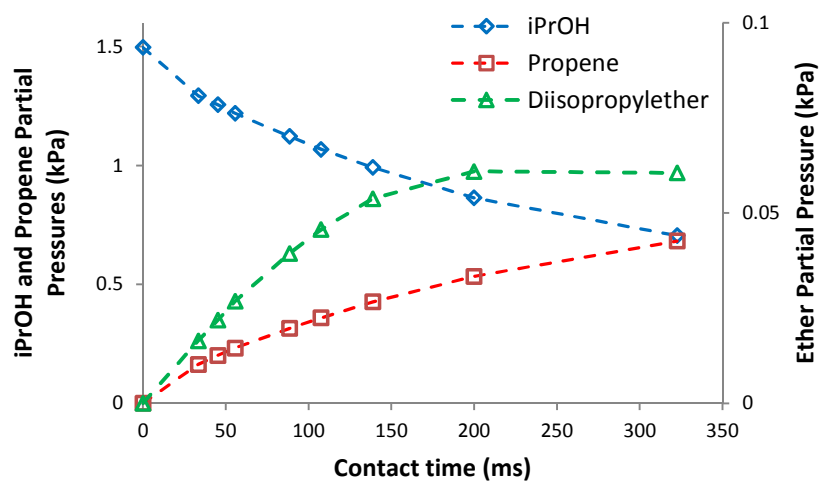
Figure S7. Partial pressures evolution on $NaNO_3$ poisoned γ-alumina (0.1 %). T_R = 200 °C, P_{iPrOH} = 1.5 kPa, m_{cata} = 80 mg.

6- Hydration state of γ-alumina according to Density Functional Theory calculations

We consider herein that the whole surface of each crystallographic plane ((100) or (110)) is composed of N elementary surface cells. Each cell behaves as a complex that can bind water molecules: 1 to 6 for the (110) crystallographic plane, and 1 to 4 for the (100) plane. Let us define the successive adsorption reactions (Si) and global adsorption reactions (Gi) :

$$H_2O_{(g)} + A_{i-1} = A_i \qquad\qquad\qquad (S_i)$$

$$i\, H_2O_{(g)} + A_0 = A_i \qquad\qquad\qquad (G_i)$$

where A_i stand for the surface cell with i water molecules attached ($0 \leq i \leq 4$ for the (100) surface, $0 \leq i \leq 6$ for the (110) surface). The associated thermodynamic constants are noted K_i^0 and β_i^0. For each of these reactions, standard enthalpies and entropies have been calculated using DFT. The results at 25 °C for reactions (S$_i$) are reported in Table S1. These values have a very small temperature-dependence over the range 0 to 750 °C. For this reason, the value at 25 °C has been employed on the whole temperature range. We emphasize here again that we used surface models for the hydrated (110) termination derived from the recent work of Wischert et al.,[7] who consider a stabilizing surface reconstruction by migration of an aluminium atom in a tetrahedral coordination. We found this phenomenon to be stabilizing for OH coverage from 9.0 to 15.0 OH.nm^{-2}.

From these data, reaction constants can be calculated. The following equations lead to the values of the proportions x_i of cells occupied by i water molecules, as a function of the temperature, for a given water partial pressure P_{H2O} at equilibrium.

$$K_i^0 = \frac{x_i}{x_{i-1} P_{H2O}} \qquad\qquad\qquad (S7)$$

$$\beta_i^0 = \frac{x_i}{x_0 (P_{H2O})^i} \qquad\qquad\qquad (S8)$$

$$\beta_i^0 = \prod_{n=1}^{i} K_n^0 \qquad\qquad\qquad (S9)$$

$$\sum_{i=0}^{i_{max}} x_i = 1 \qquad\qquad\qquad (S10)$$

$$x_i = \frac{\beta_i^0 (P_{H2O})^i}{\sum_{i=0}^{imax} \beta_i^0 (P_{H2O})^i} \qquad \text{and} \qquad x_0 = \frac{1}{\sum_{i=0}^{imax} \beta_i^0 (P_{H2O})^i} \qquad \textbf{(S11)}$$

Table S2. Successive computed enthalpies and entropies of adsorption of water on both surfaces at 25 °C. Entropies are given in $J.K^{-1}.mol^{-1}$ and enthalpies in $kJ.mol^{-1}$. The corresponding OH coverage is given in $OH.nm^{-2}$. Note that the number of adsorbed molecules is the number of molecules adsorbed on the elementary surface cell; as our periodic simulation cell contains 4 elementary cells, the simulation cell contains *4 i* water molecules.

| (110)	1	2	3	4	5	6
$\Delta_{ads}H°$	-228	-196	-167	-135	-69	-54
$\Delta_{ads}S°$	-148	-186	-158	-165	-167	-163
OH coverage	3.0	5.9	8.9	11.8	14.8	17.7
(100)	1	2	3	4		
$\Delta_{ads}H°$	-100	-110	-89	-60		
$\Delta_{ads}S°$	-157	-169	-176	-143		
OH coverage	4.3	8.6	12.9	17.2		

7- <u>**Energetic span concept**</u>

Let us consider the following situation:

- B is a reactant that may lead to products P through an activated complex T;
- B is in rapid equilibrium with another species A, and the formation of A from B is poorly activated. A is more stable than B.

We thus define the constants k_1 and $K°$ for the reactions :

$$B \rightarrow P \qquad\qquad k_1 = \frac{k_B T}{h} \exp\left(-\frac{\Delta_r G_1^{\ddagger}}{RT}\right)$$

$$B = A \qquad\qquad K^0 = \exp\left(-\frac{\Delta_r G^0}{RT}\right) = \frac{[A]}{[B]}$$

The situation can be represented on a Gibbs free energy diagram as follow:
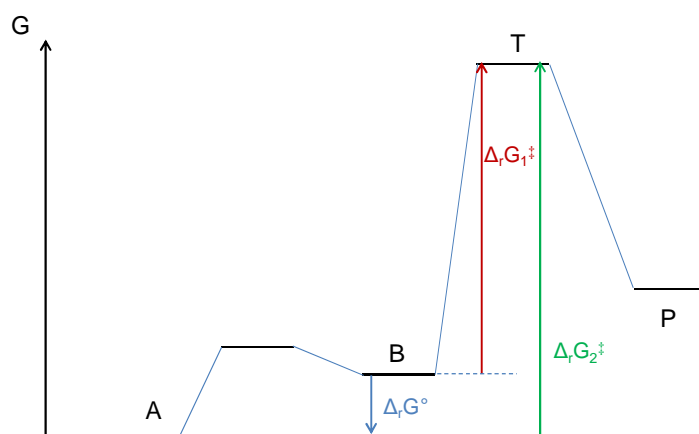
We call $C°$ the total concentration in A and B, such as $[A] + [B] = C°$. We express $[A]$ and $[B]$ as a function of $K°$ and $C°$:

$$[A] = \frac{K^0}{1 + K^0} C^0 \qquad \text{and} \qquad [B] = \frac{1}{1 + K^0} C^0$$

If A is more stable than B to the extent that $K° \gg 1$, we simplify those relations:

$$[A] \simeq C^0 \qquad \text{and} \qquad [B] \simeq \frac{C^0}{K^0}$$

and of course $[A] \gg [B]$. The main consequence of these equations is that the concentration of B strongly depends on the temperature, while the concentration of A does not (at least less than $[B]$). As a result, the reaction rate temperature dependence depends on both on the activation enthalpy $\Delta_r H_1^{\ddagger}$ and on the standard enthalpy $\Delta_r H^0$:

The reaction rate for the formation of the products P can be expressed as

$$r = k_1[B] \simeq k_1 \frac{C^0}{K^0} = \frac{k_B T}{h} \exp\left(-\frac{\Delta_r G_1^{\ddagger}}{RT}\right) \frac{C^0}{K^0}$$

The experimental activation enthalpy is determined by plotting $\ln(r/T)$ as a function of $1/T$. Let us calculate this expression (Eyring plot):

$$\ln\left(\frac{r}{T}\right) = \ln\left(\frac{k_1[B]}{T}\right) \simeq \ln\left(\frac{k_B C^0}{h}\right) - \left(\frac{\Delta_r G_1^{\ddagger}}{RT}\right) - \ln(K^0)$$

$$\ln\left(\frac{r}{T}\right) \simeq \ln\left(\frac{k_B C^0}{h}\right) - \left(\frac{\Delta_r G_1^{\ddagger}}{RT}\right) + \left(\frac{\Delta_r G^0}{RT}\right)$$

$$= \ln\left(\frac{k_B C^0}{h}\right) + \left(\frac{\Delta_r S_1^{\ddagger} - \Delta_r S^0}{R}\right) - \left(\frac{\Delta_r H_1^{\ddagger} - \Delta_r H^0}{RT}\right)$$

Thus, plotting $\ln(r/T)$ *vs.* $1/T$ yields a straight line with the slope a

$$a = -\left(\frac{\Delta_r H_1^{\ddagger} - \Delta_r H^0}{R}\right) = -\left(\frac{\Delta_r H_2^{\ddagger}}{R}\right)$$

if we define $\Delta_r H_2^{\ddagger}, \Delta_r S_2^{\ddagger}, \Delta_r G_2^{\ddagger}$ and k_2 such as:

$$\Delta_r G_2^{\ddagger} = \Delta_r G_1^{\ddagger} - \Delta_r G^0$$
$$\Delta_r H_2^{\ddagger} = \Delta_r H_1^{\ddagger} - \Delta_r H^0$$
$$\Delta_r S_2^{\ddagger} = \Delta_r S_1^{\ddagger} - \Delta_r S^0$$
$$k_2 = \frac{k_B T}{h} \exp\left(-\frac{\Delta_r G_2^{\ddagger}}{RT}\right) = \frac{k_1}{K^0}$$

We may rewrite the Eyring plot accordingly:

$$\ln\left(\frac{r}{T}\right) \simeq \ln\left(\frac{k_B C^0}{h}\right) + \left(\frac{\Delta_r S_2^{\ddagger}}{R}\right) - \left(\frac{\Delta_r H_2^{\ddagger}}{RT}\right)$$

and the rate expression :

$$r = k_1[B] \simeq k_1 \frac{C^0}{K^0} = k_2 C^0 \simeq k_2[A]$$

which is exactly the rate expression for reaction A → P.

As a conclusion, in such a case, the temperature dependence of the rate is determined by the enthalpic difference between the transition state T and the most stable species (A), and not between T and the less stable species B - although this latter is likely to be closer in structure to the activated complex than A. This relates to the TOF-determining transition state (TDTS) and the TOF-determining intermediate (TDI) in the energetic span concept.[8,9] In other words, the rate reflects the population of the possible initial states, and thus the most abundant species is the most relevant as the initial state.

In the case encountered in the manuscript, A is the dissociated state on the Al_{Va} aluminum site of the (100) surface, while B is the associated alcohol. The calculated parameters are

- $\Delta_r H° = -10$ kJ.mol^{-1}
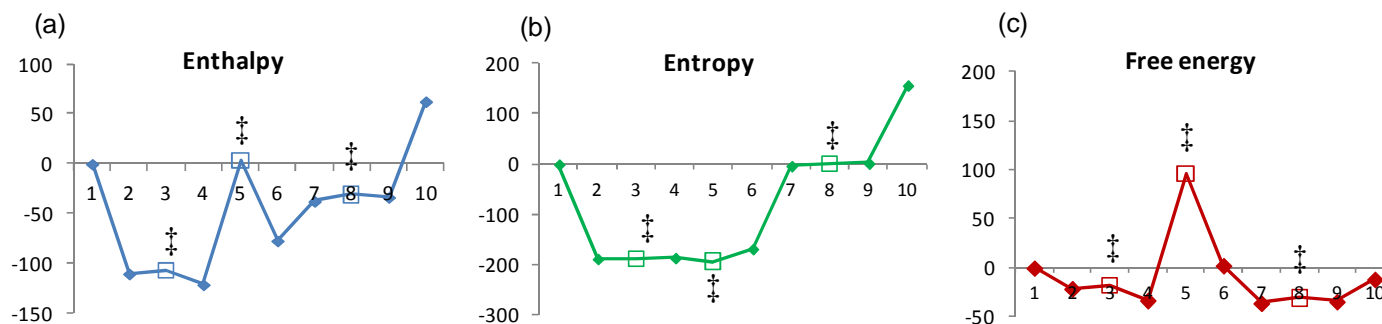- $\Delta_r S° = 2$ J.K^{-1}.mol^{-1}
- $K° = 16.2$

This yields $[A]/C^0 = 0.94$ and $[B]/C^0 = 0.06$. 94 % of the total occupied sites is in the dissociated form while only 6 % remain under the associated form.

For these reasons, we chose to consider the dissociated form as the common initial state for every calculated activation parameter on this site.

8- Thermodynamic functions evolutions along the reaction paths
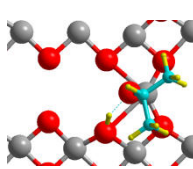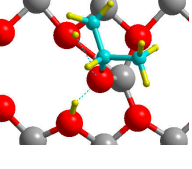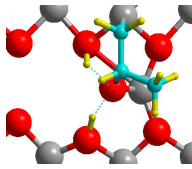
8.1. Formation of propene

E2 mechanism
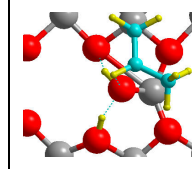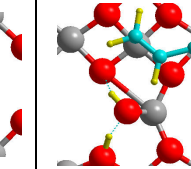
Step N°	1	2	4	5‡	6	7	9	10
Surface species								
Gas-phase species	*i*PrOH	-	-	-	-	Propene	Propene	H₂O + Propene
Chemical nature of the step	*Isopropanol adsorption*		*Isopropanol dissociation*	*Concerted formation of propene (abstraction of Hβ and breaking of C-O bonds)*		*Desorption of propene*	*Recombination of water*	*Desorption of water*

Figure S8. Evolution of the thermodynamic functions along the reaction pathway for the formation of propene through E2 mechanism calculated by DFT at 200 °C with respect to the reference state {surface + *i*PrOH$_{(g)}$}(site Al$_{Va}$; surface (100)) (a) Enthalpy (kJ.mol^{-1}) (b) Entropy (J.K^{-1}.mol^{-1}) (c) Gibbs free energy (kJ.mol^{-1}). The corresponding structures are shown in the table above. As indicated in the manuscript, dissociation of isopropanol (steps 2 → 4) and reassociation of the water molecule (steps 7 → 9) are very poorly activated processes. The corresponding transition states (3 and 8), which are very close in structure to the initial (or final, respectively) associated forms, are not presented here.
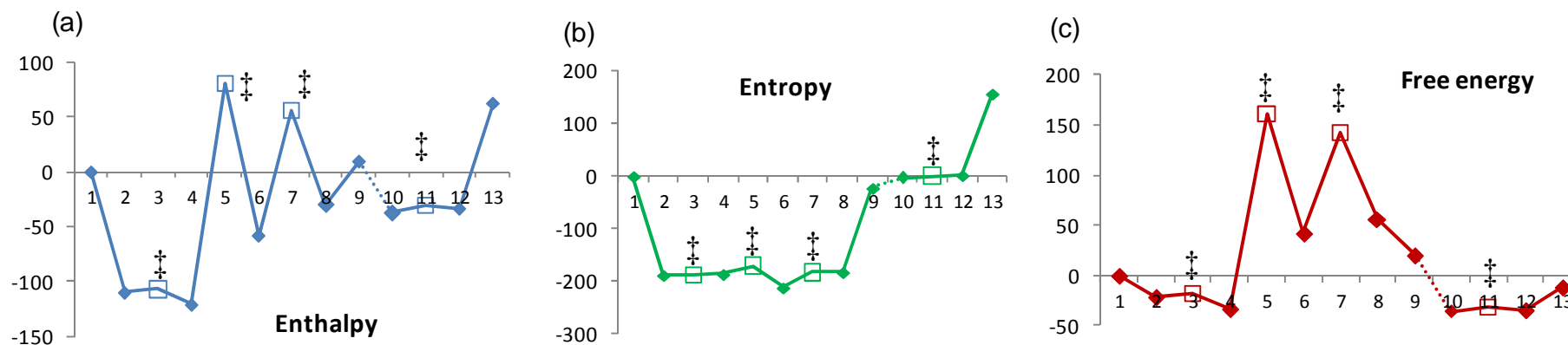
E1$_{cb}$ mechanism

Figure S9. Evolution of the thermodynamic functions along the reaction pathway for the formation of propene through E1$_{cb}$ mechanism calculated by DFT at 200 °C with respect to the reference state {surface + iPrOH$_{(g)}$}(site Al$_{Va}$; surface (100)) (a) Enthalpy (kJ.mol^{-1}) (b) Entropy (J.K^{-1}.mol^{-1}) (c) Gibbs free energy (kJ.mol^{-1}). The corresponding structures are shown in the table. Steps 1 to 4 and 9 to 12 are similar to steps 1 to 4 and 7 to 10 of the E2 mechanism.
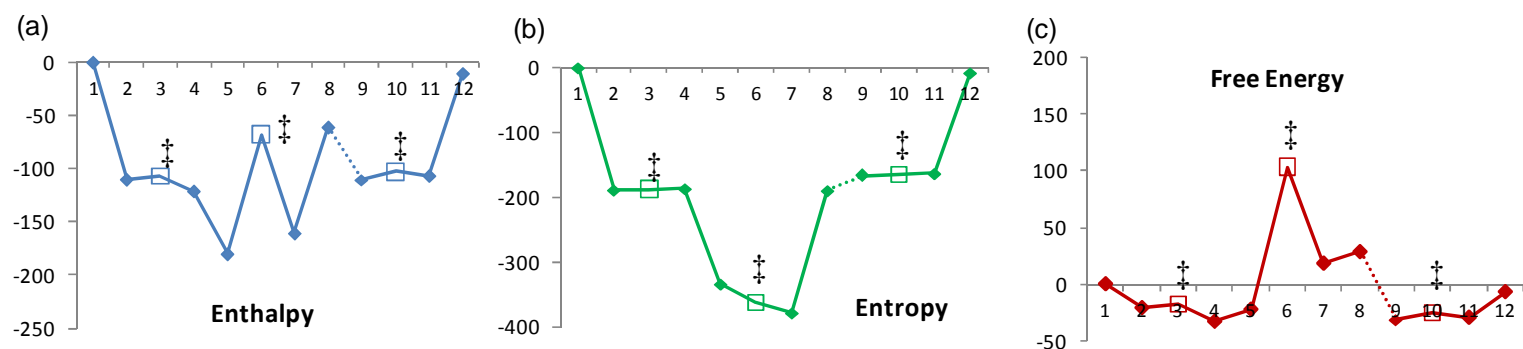
E1 mechanism

Step N°	4	5‡	6	7‡	8	9	10
Surface species							
Gas-phase species	-	-	-	-	-	Propene	Propene
Chemical nature	*Formation of a carbocation intermediate (breaking of the C-O bond)*			*Formation of propene (breaking of the C-H$_\beta$ bond)*		*Desorption of propene*	*Hydrogen transfer on the surface*	

Figure S10. Evolution of the thermodynamic functions along the reaction pathway for the formation of propene through E1 mechanism calculated by DFT at 200 °C with respect to the reference state {surface + *i*PrOH$_{(g)}$}(site Al$_{Va}$; surface (100)) (a) Enthalpy (kJ.mol^{-1}) (b) Entropy (J.K^{-1}.mol^{-1}) (c) Gibbs free energy (kJ.mol^{-1}). The corresponding structures are shown in the table. Steps 1 to 4 and 9 to 12 are similar to steps 1 to 4 and 7 to 10 of the E2 mechanism. After desorption of the propene molecule, the surface is left with a dissociated water molecule in a highly unfavourable state (step 9). We consider the stabilizing transfer of the proton from one oxygen atom to the next one to be a fast, non activated step, and thus did not calculate any transition state corresponding to the step 9 → 10 (dotted).
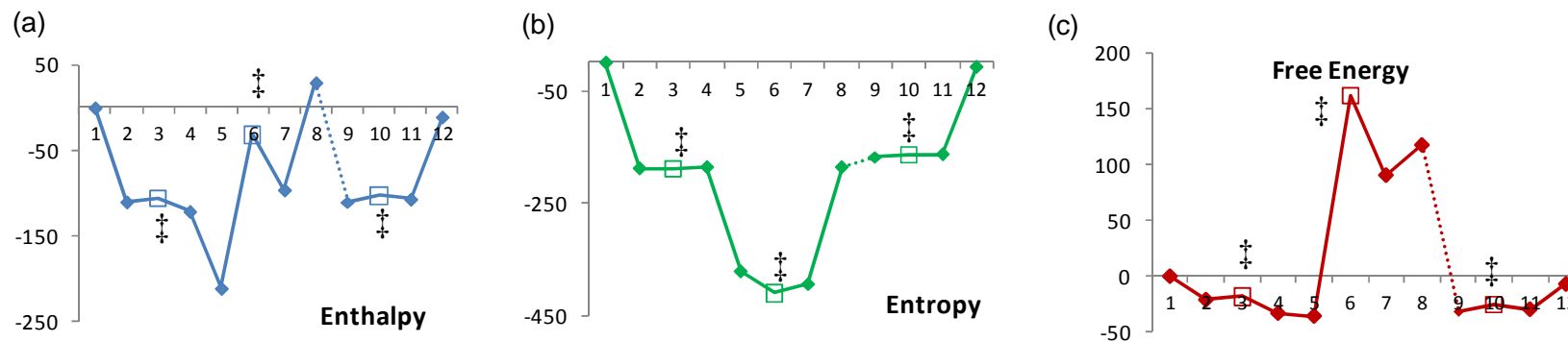
8.2.　Formation of diisopropylether

'Al$_{Va}$ – O$_{3a}$' Mechanism'

Step N°	1	4	5	6‡	7	8	9
Surface species							
Gas-phase species	2 iPrOH	iPrOH	-	-	-	Diisopropylether	Diisopropylether
Chemical nature	Adsorption of isopropanol 1 on Al$_{Va}$ + dissociation	Adsorption of isopropanol 2 on O$_{3b}$	Concerted formation of diisopropylether			Desorption of diisopropylether	Hydrogen transfer on the surface

Figure S11. Evolution of the thermodynamic functions along the reaction pathway for the formation of diisopropylether through the 'Al$_{Va}$ – O$_{3a}$' mechanism' calculated by DFT at 200 °C with respect to the reference state {surface + 2 *i*PrOH$_{(g)}$}(site Al$_{Va}$; surface (100)) (a) Enthalpy (kJ.mol^{-1}) (b) Entropy (J.K^{-1}.mol^{-1}) (c) Gibbs free energy (kJ.mol^{-1}). The corresponding structures are shown in the table. Steps 1 to 4 are similar to steps 1 to 4 of the E2 mechanism, with one additional isopropanol molecule in the gas phase. Steps 10 to 13 are similar to steps 7 to 10 of the E2 mechanism, although with diisopropylether in the gas phase instead of propene. After desorption of the diisopropylether molecule, the surface is left with a dissociated water molecule in a highly unfavourable state (step 8). We consider the stabilizing transfer of the proton from one oxygen atom to the next one to be a fast, non activated step, and thus did not calculate any transition state corresponding to the step 8 → 9 (dotted).
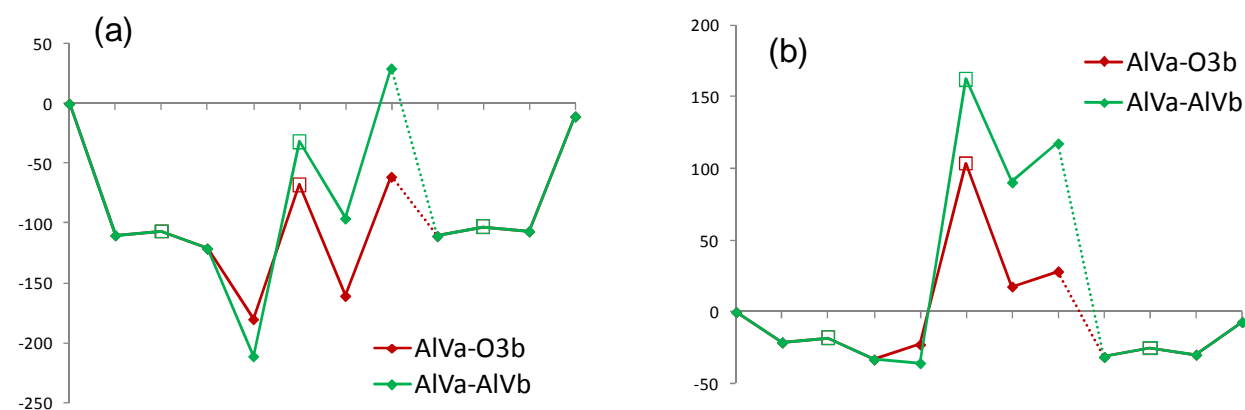
'Al$_{Va}$ - Al$_{Vb}$ Mechanism'

Step N°	4	5	6‡	7	8	9
Surface species						
Gas-phase species	*i*PrOH	-	-	-	Diisopropylether	Diisopropylether
Chemical nature	*Adsorption of isopropanol 2 on Al$_{Vb}$*	*Concerted formation of diisopropylether*			*Desorption of diisopropylether*	*Hydrogen transfer on the surface*

Figure S12. Evolution of the thermodynamic functions along the reaction pathway for the formation of diisopropylether through the 'Al$_{Va}$ – Al$_{Vb}$ mechanism' calculated by DFT at 200 °C with respect to the reference state {surface + 2 *i*PrOH$_{(g)}$}(surface (100)) (a) Enthalpy (kJ.mol^{-1}) (b) Entropy (J.K^{-1}.mol^{-1}) (c) Gibbs free energy (kJ.mol^{-1}). The corresponding structures are shown in the table. Steps 1 to 4 are similar to steps 1 to 4 of the E2 mechanism, with one additional isopropanol molecule in the gas phase.. Steps 10 to 13 are similar to steps 7 to 10 of the E2 mechanism, although with diisopropylether in the gas phase instead of propene. After desorption of the diisopropylether molecule, the surface is left with a dissociated water molecule in a highly unfavourable state (step 8). We consider the stabilizing transfer of the proton from one oxygen atom to the next one to be a fast, non activated step, and thus did not calculate any transition state corresponding to the step 8 → 9 (dotted).

8.3.   Comparison between the mechanisms
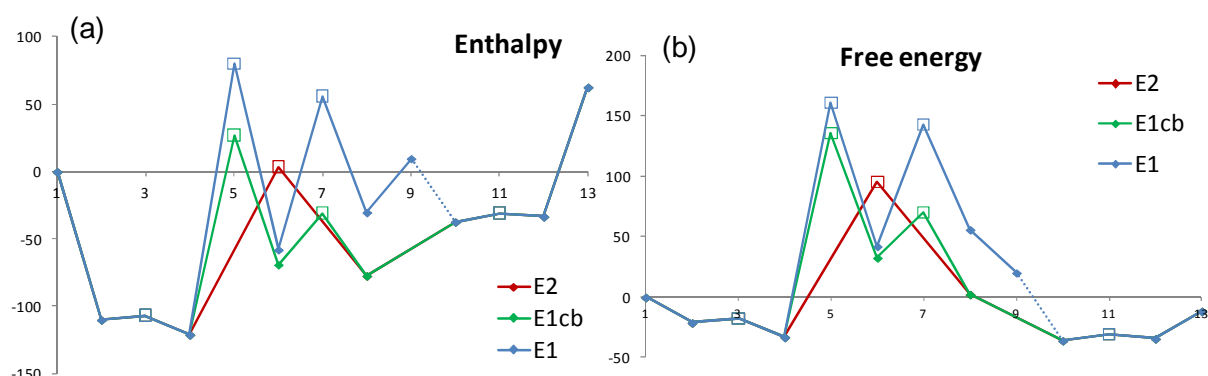
Figure S13. Comparison of the E2, E1$_{cb}$ and E1 mechanisms for the formation of propene on site Al$_{Va}$ of the (100) facets of gamma-alumina in terms of (a) Enthalpy (kJ.mol^{-1}) (b) Gibbs free energy (kJ/mol^{-1}).

Figure S14. Comparison of the mechanisms 'Al$_{Va}$-O$_{3b}$' and 'Al$_{Va}$-Al$_{Vb}$' for the formation of diisopropylether on the (100) facets of gamma-alumina in terms of (a) Enthalpy (kJ.mol^{-1}) (b) Gibbs free energy (kJ/mol^{-1}).
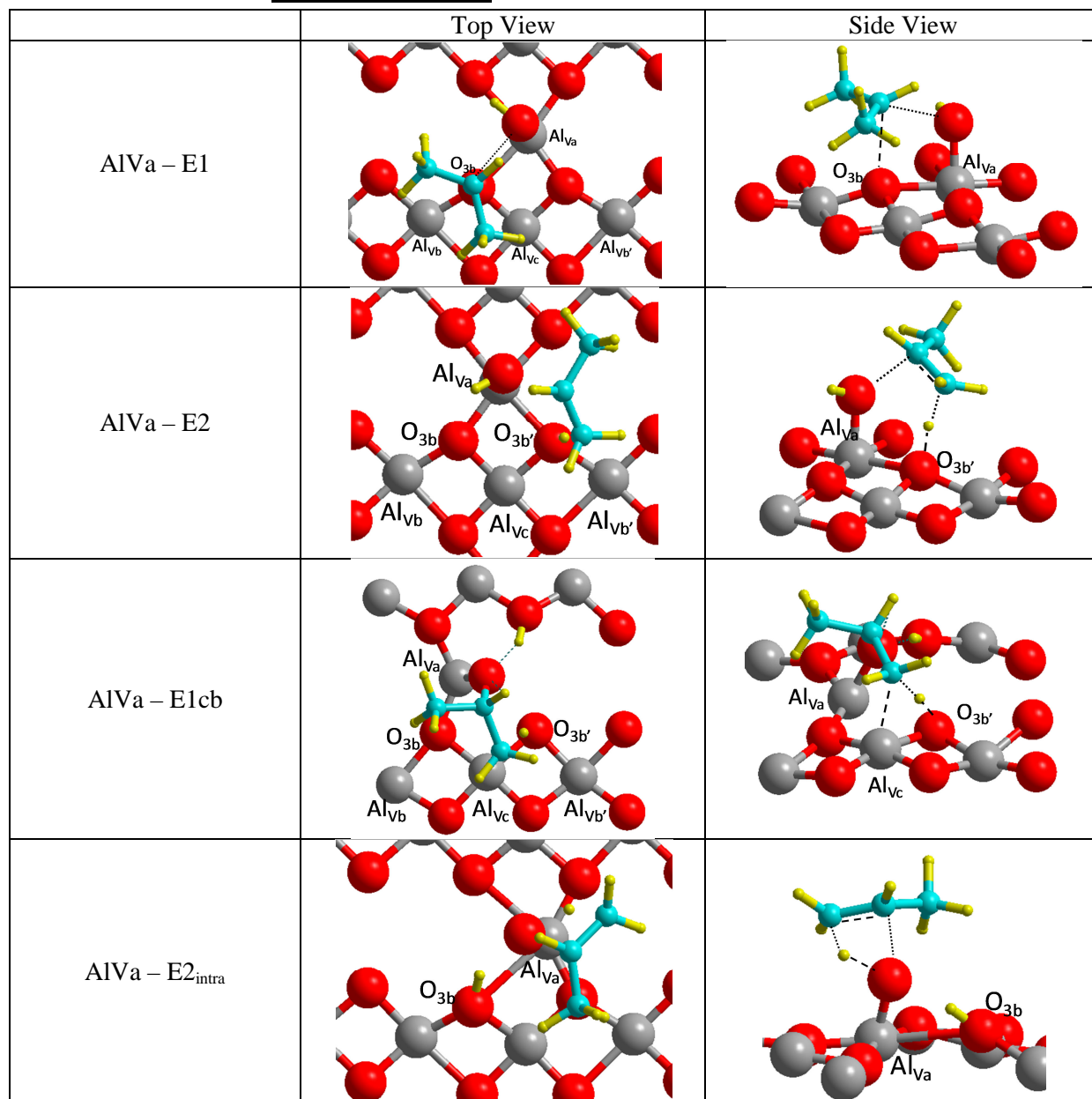
Note : In any case, the rate determining step – which is the step associated to the highest change in Gibbs free energy – is the formation of a transition state, and not a desorption step.
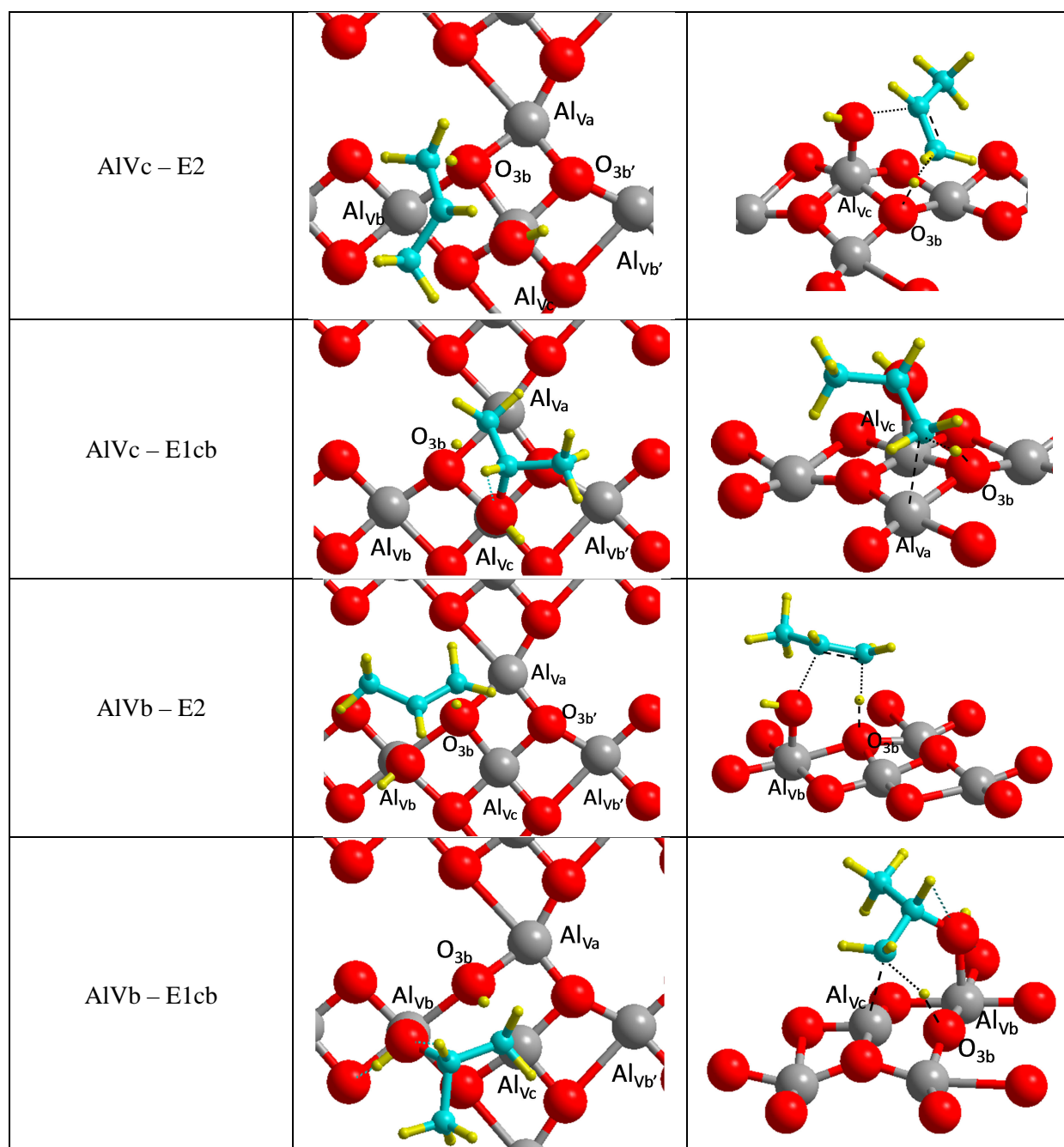
9- Transition states structures

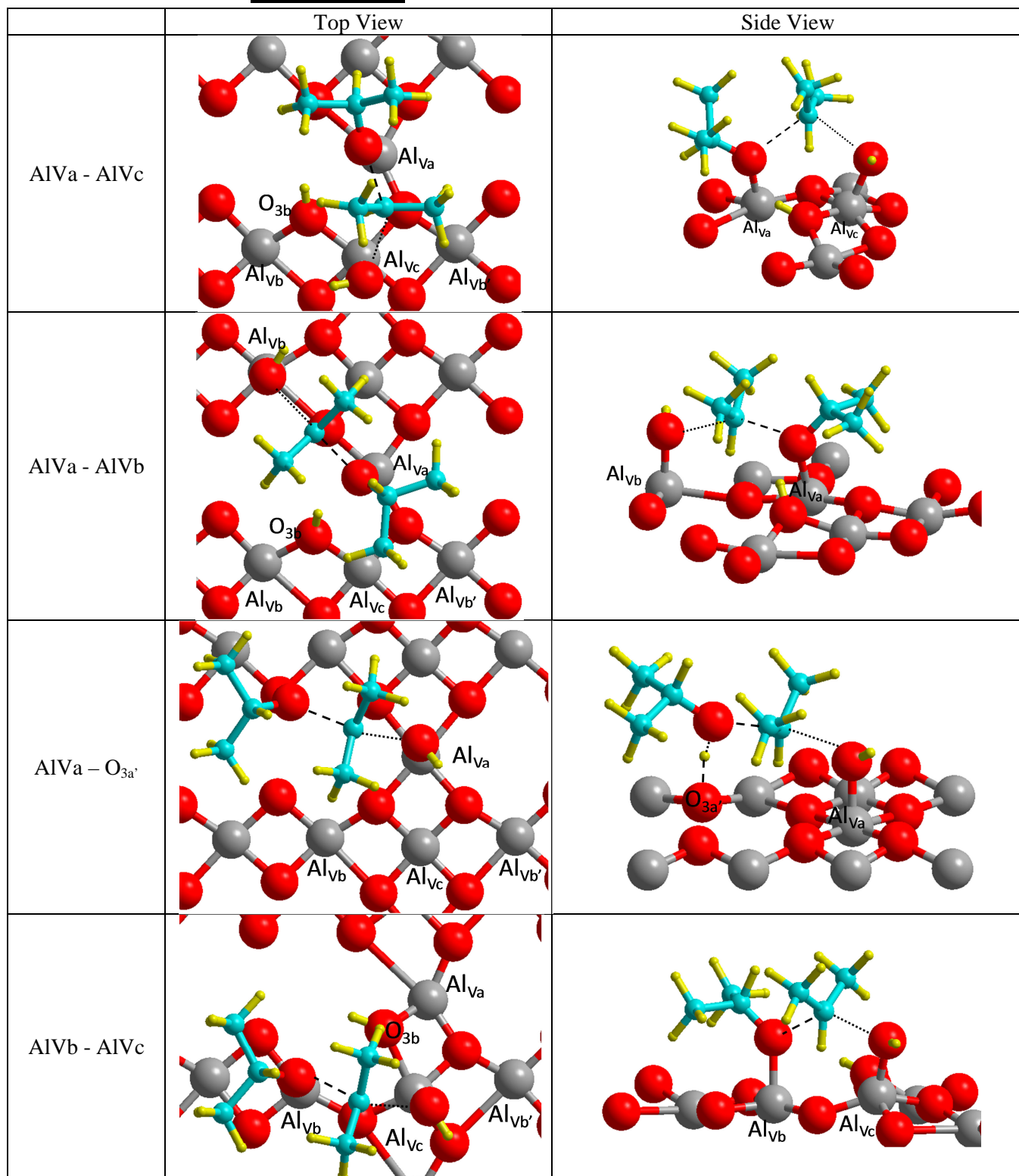In this section, - - - - represents a forming bond, while ⋯⋯ represents a breaking bond.

9.1.   (100) – propene

	Top View	Side View
AlVa – E1		
AlVa – E2		
AlVa – E1cb		
AlVa – E2$_{intra}$		

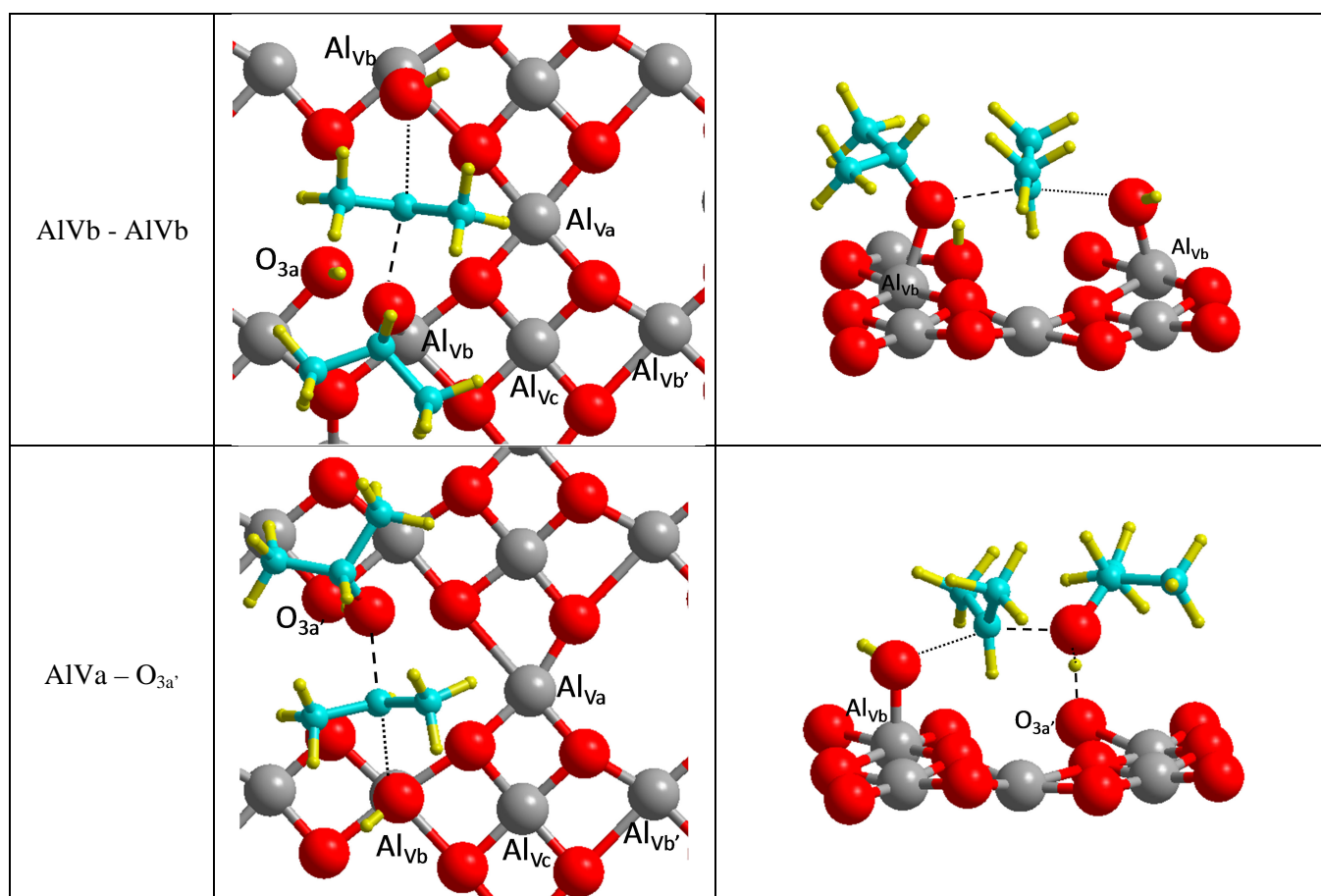|		
AlVc – E2		
AlVc – E1cb		
AlVb – E2		
AlVb – E1cb		

Figure S15. Activated complexes for the formation of propene on the (100) dehydrated surface

9.2.   (100) - Ether

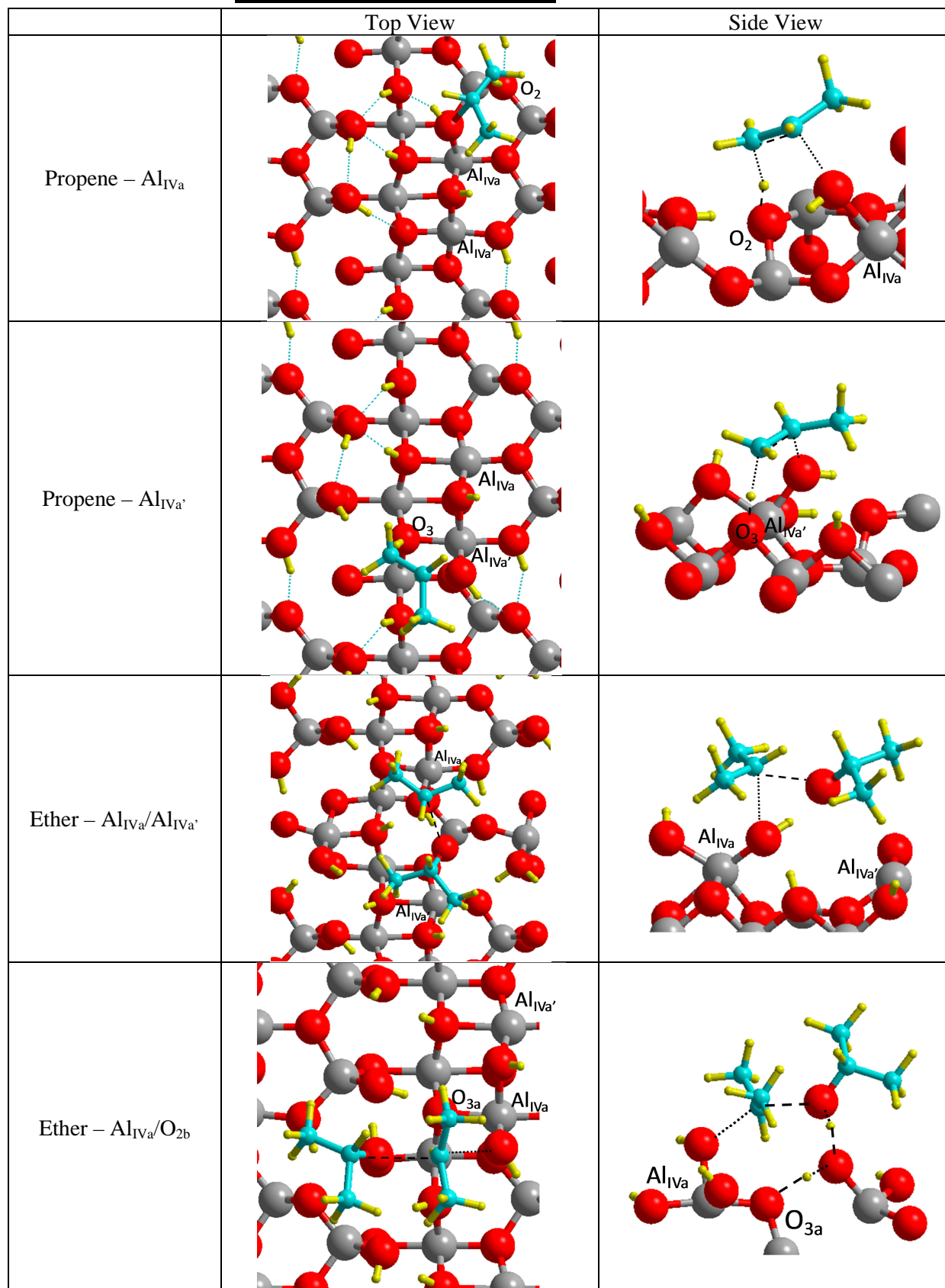|	Top View	Side View
AlVa - AlVc		
AlVa - AlVb		
AlVa – O$_{3a'}$		
AlVb - AlVc		

Figure S16. Activated complexes for the formation of diisopropylether on the (100) dehydrated surface

9.3.   (110) – Propene and Ether

	Top View	Side View
Propene – Al$_{IVa}$		
Propene – Al$_{IVa'}$		
Ether – Al$_{IVa}$/Al$_{IVa'}$		
Ether – Al$_{IVa}$/O$_{2b}$		

**Figure S17.** Activated complexes for the formation of diisopropylether and propene on the (110) hydrated surface (8.9 OH.nm^{-2})

9.4. **Miscellaneous**

	TopView	Side View
Formation of propene, Brønsted mechanism (100) surface – 8.8 OH.nm^{-2}		
Diisopropylether conversion (100) surface, site Al$_{Va}$		
Formation of propene where Al$_{III}$-μ_1OH acts as a basic center for the abstraction of the β hydrogen atom – (110) surface, 8.9 OH.nm^{-2}, surface from ref [10]		
Formation of propene where Al$_{Va}$-μ_1OH acts as a basic center for the abstraction of the β hydrogen atom – (100) surface, 4.4 OH.nm^{-2}		

Figure S18. Miscellaneous activated complexes

## 9.5. Activated complex in the presence of a coadsorbed (Na$^+$,OH$^-$) or H$_2$O species
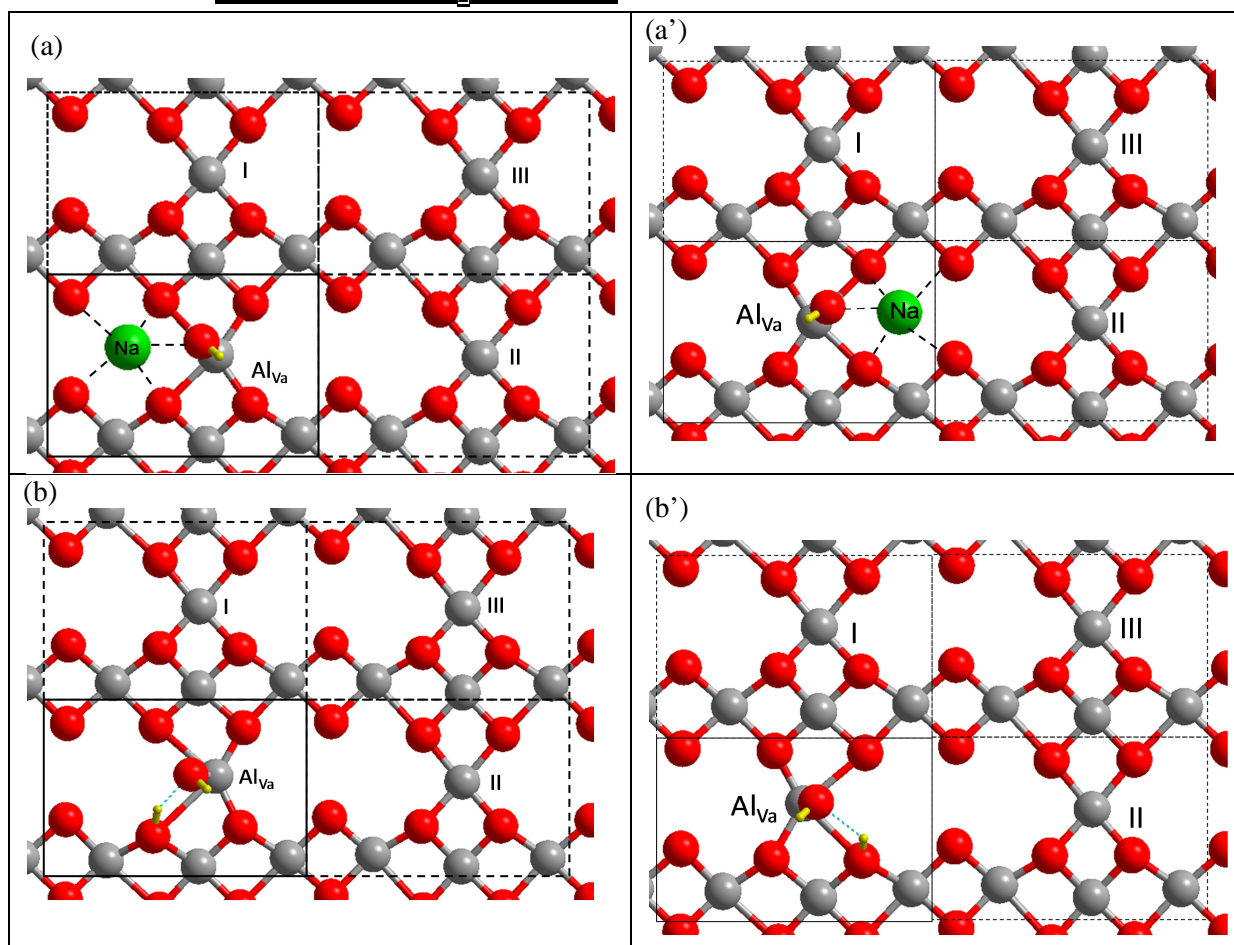
Figure S19. (100) termination with adsorbed molecule (a) and (a') NaOH ; (b) and (b') H$_2$O.
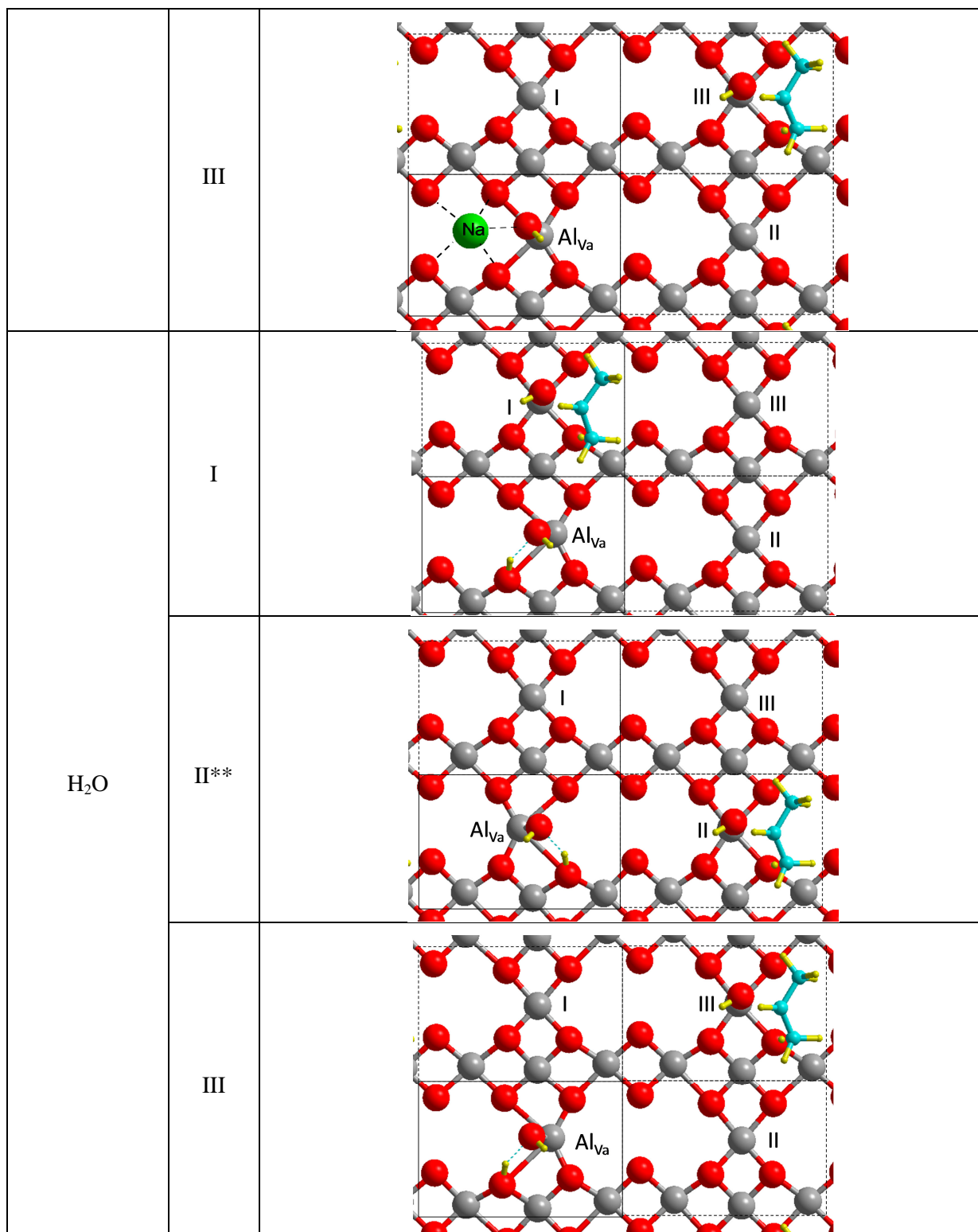
Remarks:

- (a) and (a') have symmetrical structures and identical energies,
- (b) and (b') have symmetrical structures and identical energies.

Table S3. Adsorption enthalpies and activation parameters for the formation of propene on the Al_{Va} site of the (100) terminations with NaOH or H_2O co-adsorbed molecules.

Coadsorbed molecule	Site	Adsorption		Reactivity	
		Mode	$\Delta_{ads}H°$	$\Delta_rH^{\ddagger}$	$\Delta_rS^{\ddagger}$
None	-	Dissociated	-121	125	–8
Na^+,OH^-	I	Associated	-111	120	-16
	II	Dissociated	-119	125	4
	III	Dissociated	-120	126	9
H_2O	I	Associated	-110	123	-16
	II	Associated	-112	120	-15
	III	Dissociated	-121	120	-9

Co-adsorbed molecule	Site	Activated complex
(Na^+,OH^-)	I	
	II*	

	III	
H₂O	I	
	II**	
	III	
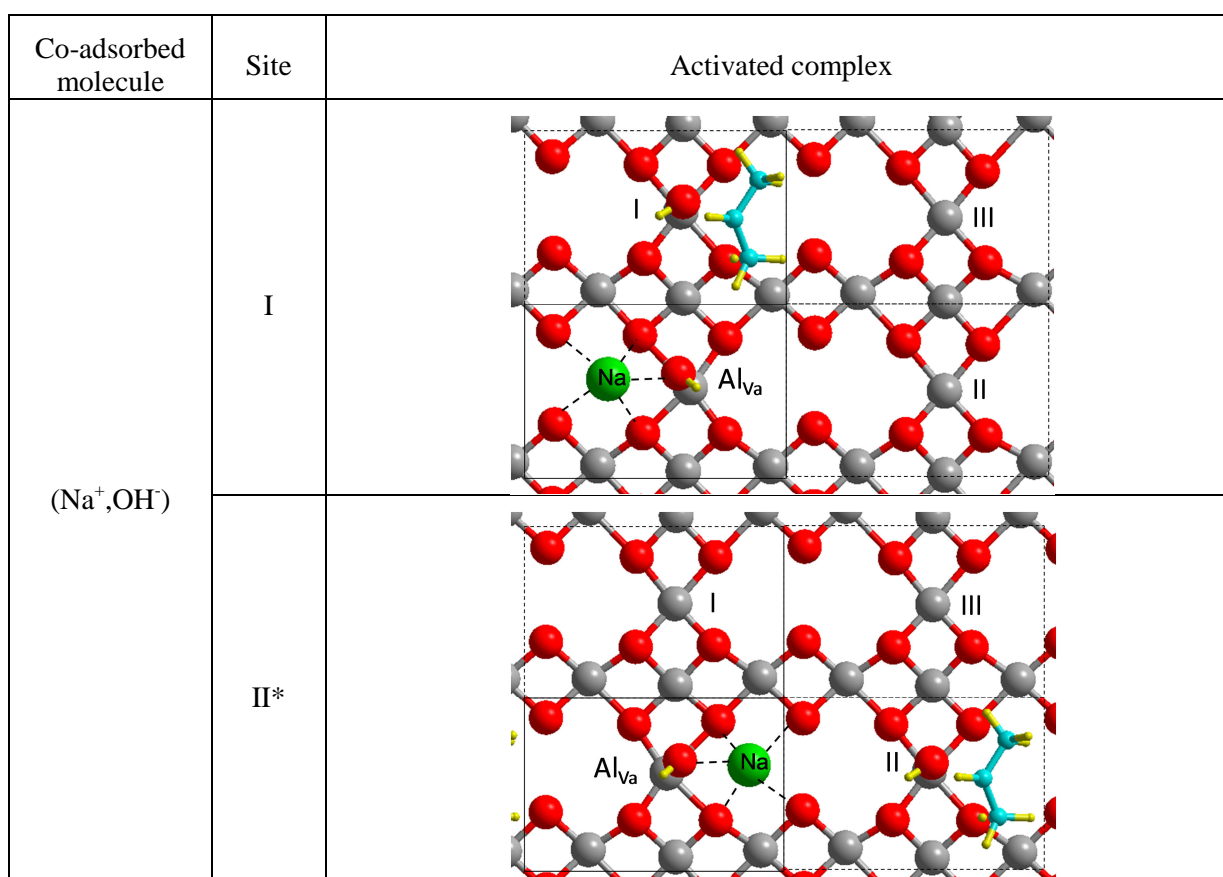
Figure S20. Activated complexes for the formation of propene from isopropanol on the (100) terminations with co-adsorbed molecules (Na$^+$, OH$^-$) or H_2O.

Remarks :
* For model II, the (a') surface model was employed in order to avoid direct steric interaction between the sodium ion and the isopropanol molecule.
** As for the co-adsorbed NaOH species, the symmetrical structure (b') was employed (see caption of Figure S12).

REFERENCES

(1)   Delgado, J. M. P. Q. *Heat Mass Transf.* **2006**, *42*, 279–310.

(2)   Sackur, O. *Ann. Phys.* **1913**, *345*, 67–86.

(3)   Tetrode, H. *Ann. Phys.* **1912**, *343*, 434–442.

(4)   De Moor, B. A.; Reyniers, M.-F.; Marin, G. B. *Phys. Chem. Chem. Phys.* **2009**, *11*, 2794–2798.

(5)   Canduela-Rodriguez, G.; Sabbe, M. K.; Reyniers, M.-F.; Joly, J.-F.; Marin, G. B. *Phys. Chem. Chem. Phys.* **2014**, *16*, 23754–23768.

(6)   CHEMKIN-PRO 15131, Reaction Design, San Diego, 2013.

(7)   Wischert, R.; Laurent, P.; Copéret, C.; Delbecq, F.; Sautet, P. *J. Am. Chem. Soc.* **2012**, *134*, 14430–14449.

(8)   Amatore, C.; Jutand, A. *J. Organomet. Chem.* **1999**, *576*, 254–278.

(9)   Kozuch, S.; Shaik, S. *Acc. Chem. Res.* **2011**, *44*, 101–110.

(10)   Digne, M.; Sautet, P.; Raybaud, P.; Euzen, P.; Toulhoat, H. *J. Catal.* **2002**, *211*, 1–5.